Design and synthesis of novel hybrid metal complex–DNA conjugates: key building blocks for multimetallic linear DNA nanoarrays†

Sumana Ghosh,[a] Isabelle Pignot-Paintrand,[b] Pascal Dumy[a] and Eric Defrancq*[a]

We describe here a short and efficient synthetic route for incorporating terpyridine based metal complexes at the 3′-extremity of both single and bis-oligonucleotide (bis-ODN) stretches to form novel metal complex–ODN conjugates. All single stranded mono and bis-ODN tethered metal complexes and the respective duplex ODNs were characterized by circular dichroism spectroscopy and UV-Vis melting experiments. Duplexes formed by these hybrid metal complex–DNA conjugates showed around 4–5 °C stabilization with respect to the unmodified duplexes. Moreover hybridization of two complementary bis-ODN tethered metal complexes at different ratios in solution gave rise to a self-assembled nanometric linear network, which was characterized by non-denaturing gel electrophoresis and TEM studies. Thus, our simple synthetic strategy would contribute to develop multimetallic 2D-DNA nanoarrays where we can place different metal complexes at regular intervals along the ODN stretches.

Introduction

A major challenge of the "bottom-up" strategies for the design of nanomaterials is the construction of complex architectures from nanoscale building blocks. The self-assembly process is one of the key elements for building such nanostructures and nanodevices. Indeed, the exact spatial positioning of materials is crucial for the future development of structured nanodevices. In this context, DNA has emerged as a promising candidate due to its nanometric dimensions and highly selective self-assembly behavior *via* its programmable hybridization properties.[1] Another advantage of using DNA as a structural scaffold for nanostructure design is its efficient access *via* automated solid phase synthesis. In fact, any kind of base ordering with different lengths and base modifications can be achieved quite quantitatively (almost on a microgram scale) within a short time period. Since pioneering work by Seeman,[2] many interesting programmable DNA self-assemblies have been prepared starting from simple linear networks to three-dimensional (3D) nanostructures.[3]

In this way, DNA-programmed assembly of inorganic building blocks is of great interest for photo- and electrochemical devices as DNA can act as a template to organize the inorganic molecular units to provide nanometre-scale features and patterns for the system. The metal complexes can influence both structure and function of the DNA nanostructures due to their varied coordination nature (tetrahedral to octahedral to square planar *etc.*) as well as their different redox, photochemical and catalytic properties.

In this context, different metal complexes have been tethered to oligonucleotides to prepare self-assembled nanostructures upon hybridization with appropriate complementary ODN sequences.[4] One of the critical steps for further development of such nano-materials concerns the availability of the starting building-blocks, *i.e.* the metal complex–oligonucleotide conjugates. During the last decade, great efforts have been devoted to new methods for an efficient incorporation of reporters into the oligonucleotides and more recently have resulted in the development of the "Click Chemistry concept".[5] Among the various proposed strategies, the Huisgens cycloaddition has received particular attention as the involved functional groups have shown good compatibility with DNA synthesis.[6] However, this strategy employs copper catalysis, which could complicate conjugation with the respective metal moieties.

In this paper, we describe our contribution to building linear DNA networks with two metal ions (Fe(II) and Ru(II)) using terpyridine as a ligand. For the incorporation of the metal complex in the oligonucleotides, we have adapted the oxime tethering procedure, initially developed for the chemoselective ligation of ODNs with carbohydrates, peptides and glycopeptides, which further fulfilled the "Click Chemistry" criteria.[7] For this purpose, the different terpyridine-based metal complexes **1–3** containing a reactive oxyamino group were prepared and conjugated with aldehyde containing modified ODN stretches *via* the formation of an oxime linkage. Using this strategy, we were able to characterize separately both the metal complex and modified ODN before their conjugation step. Furthermore, we can avoid degradation of the metal complex from harsh conditions employed in solid phase DNA synthesis. Such a synthetically simple conjugation strategy of different ODN stretches with various metal complexes of varying optical absorption, luminescence and redox activity would arguably offer a key building block for the design of functional nanostructures.

Two types of metal–ODN based building blocks were generated from the metal complexes **1–3**: one with a homoleptic metal

[a]*Département de Chimie Moléculaire UMR CNRS 5250, Université Joseph Fourier BP 53, 38041, Grenoble Cedex 9, France. E-mail: Eric.Defrancq@ujf-grenoble.fr; Fax: +33 (0)4 76 51 49 46*
[b]*Centre de Recherches sur les Macromolécules Végétales, UPR 5301-CNRS, BP 53, F-38041, Grenoble Cedex 9, France*

complex designated as "A" and the other with a heteroleptic metal complex designated as "B" (Fig. 1). Hybridization between these building blocks at different ratios gave rise to a either trinuclear structure or linear 2D-network. All these kinds of self-assembly structures were studied by CD spectroscopy, thermal denaturation experiment and non-denaturing gel electrophoresis studies. Some evidences of the formation of long linear networks were also obtained by transmission electron microscopy.
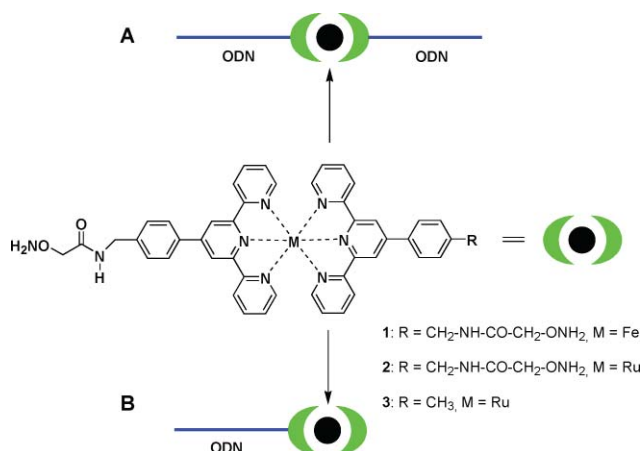

Fig. 1 Structure of homoleptic metal complexes **1** and **2** and heteroleptic metal complex **3**. Schematic representation of A/bis-ODN tethered metal complex building block and B/mono-ODN tethered metal complex building block.

Results and discussion

Ligand synthesis (Scheme 1)

The tolyl terpyridine (ttpy) derivative was chosen as the building block for preparing different metal complexes due to its
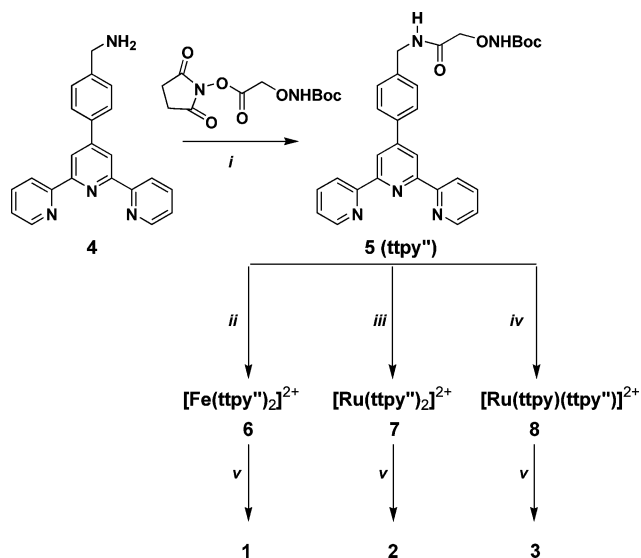
Scheme 1 *Reagents and conditions*: (i) CH_2Cl_2, RT, 6 h, (65%); (ii) Et_3N, $CHCl_3$–EtOH (1 : 2), $FeCl_2 \cdot 4H_2O$, RT, 1 h (70%); (iii) $RuCl_3 \cdot xH_2O$, $AgNO_3$, $CHCl_3$–EtOH (1 : 2), reflux, (30%); (iv) $[Ru(ttpy)Cl_3]^{2+}$, $AgNO_3$, $CHCl_3$–EtOH, reflux, 8 h, (40%); (v) CH_3CN–1 N HCl (1 : 1, v/v), RT, 2 h, (80%).

improved fluorescence properties compared to a simple terpyridine scaffold.[8] Tolyl terpyridine was converted to amino methyl terpyridine derivative **4** according to the reported procedure.[9] The oxyamino moiety was then introduced by reaction with the *N*-hydroxysuccinimide ester of *N*-Boc-*O*-(carboxymethyl)-hydroxylamine to obtain the oxyamino-protected terpyridine ligand **5** (ttpy''). This ligand was further used to prepare the different Fe(II) and Ru(II) complexes **1–3**.

For the synthesis of iron complex **1**, two equivalents of ligand **5** were reacted with ferrous chloride in ethanol in the presence of a catalytic amount of triethylamine at room temperature. The base is required to prevent the cleavage of the Boc protecting group. The reaction was completed within 10–15 min and finally violet colored complex $[Fe(ttpy'')_2]^{2+}$ **6** was formed.

The two Ru(II) complexes **7** and **8** containing either one or two oxyamine containing terpyridine moieties were also synthesized from ligand **5**. In one case, $RuCl_3 \cdot 3H_2O$ was reacted with two equivalents of ligand **5** (ttpy'') under reflux in the presence of $AgNO_3$ for 12 h. The final reaction mixture was filtered and purified by silica gel chromatography to obtain red colored homoleptic $[Ru(ttpy'')_2]^{2+}$ complex **7**. On the other hand, $RuCl_3 \cdot 3H_2O$ was first reacted with tolyl terpyridine (ttpy) in a chloroform–ethanol mixture under reflux for 12 h followed by filtration to obtain the intermediate $[Ru(ttpy)Cl_3]^{2+}$ as a red colored solid. This intermediate was used without further purification for the reaction with ligand **5** (ttpy'') under reflux in the presence of $AgNO_3$. The final reaction mixture was then filtered and the residue was purified by silica gel chromatography to give the final heteroleptic $[Ru(ttpy)(ttpy'')]^{2+}$ complex **8** as a red colored solid. All the above Fe(II) and Ru(II) complexes were characterized by ¹H-NMR, ¹³C-NMR and mass spectrometry. These Boc protected oxyamine containing metal complexes were next treated with a 1 N aqueous HCl solution for 2 h at room temperature to obtain the reactive oxyamine containing Fe(II) and Ru(II) complexes **1–3** which were used without further purification for subsequent conjugation with the aldehyde derivatized oligonucleotide stretches.

Oligonucleotide–metal complex coupling reaction (Scheme 2)

Two types of oligonucleotide (ODN) stretches were selected: the AT-rich sequence 5′-TTTTTTTATTAAATTTAX-3′ **9a** and its complementary sequence **9b**, and the GC-rich sequence 5′-ACGTGAGTTGAGACGTX-3′ **9c**, and its complementary sequence **9d**. All these sequences are 3′-modified by a 1-2 diol moiety (X represents the 3′-glyceryl modification). These ODNs were reacted with an excess of sodium periodate for 1 h at room temperature to obtain 3′-aldehyde containing ODNs **10a–d** by using a previously reported method.[10] These reactive aldehyde containing ODNs were subsequently reacted with oxyamine containing Fe(II) and Ru(II) complexes **1–3** in 0.4 M ammonium acetate buffer (pH = 4.5) and the progress of each reaction was monitored by RP-HPLC. Depending on the molar ratio between the metal complex and the aldehyde containing ODNs, we were able to achieve mono and bis-ODN conjugated metal complexes. The coupling of a single ODN strand to the reactive ruthenium metal complex **3** was very fast and within 1 h most of the modified ODNs were converted to the ruthenium–ODN hybrid conjugates **11a–d**. On the other hand, the coupling of two ODNs on either side of the metal complexes **1** and **2** required more time and within
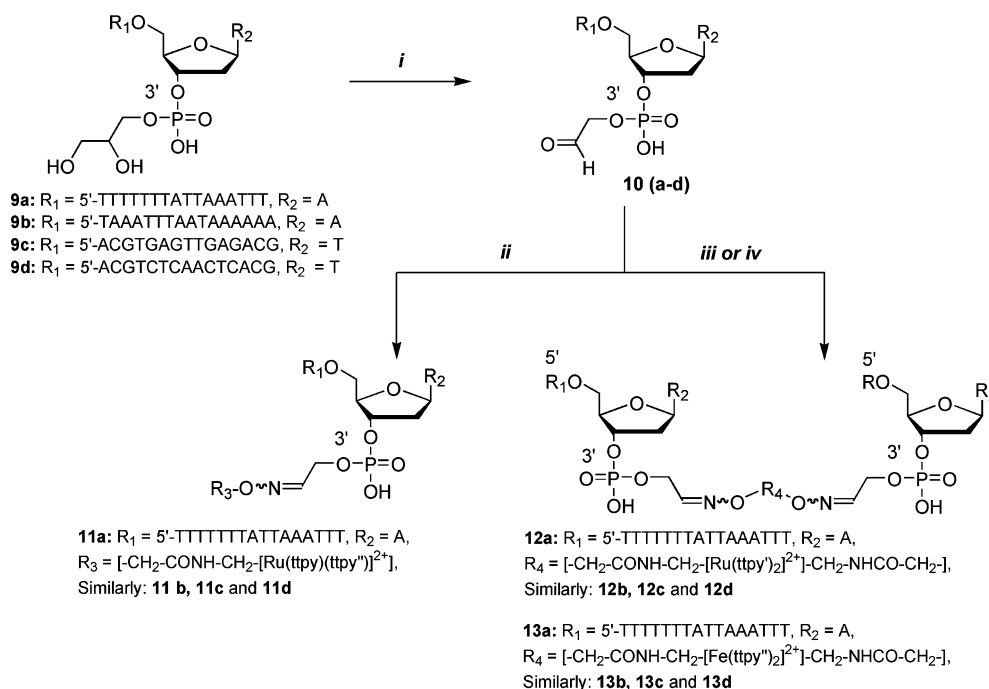
Scheme 2 *Reagents and conditions*: (i) 15 equiv. of NaIO$_4$ in H$_2$O, 1 h; (ii) 2.5 equiv. of [Ru(ttpy)(ttpy″)]$^{2+}$ **3** in 0.4 M ammonium acetate buffer, pH = 4.5, RT, 2 h, (40%); (iii) 0.5 equiv. of [Ru(ttpy″)$_2$]$^{2+}$ **2** in 0.4 M ammonium acetate buffer, pH = 4.5, RT, 2 h, (35%); (iv) 0.5 equiv. of [Fe(ttpy″)$_2$]$^{2+}$ **1** in 0.4 M ammonium acetate buffer, pH = 4.5, RT, 2 h, (35%).
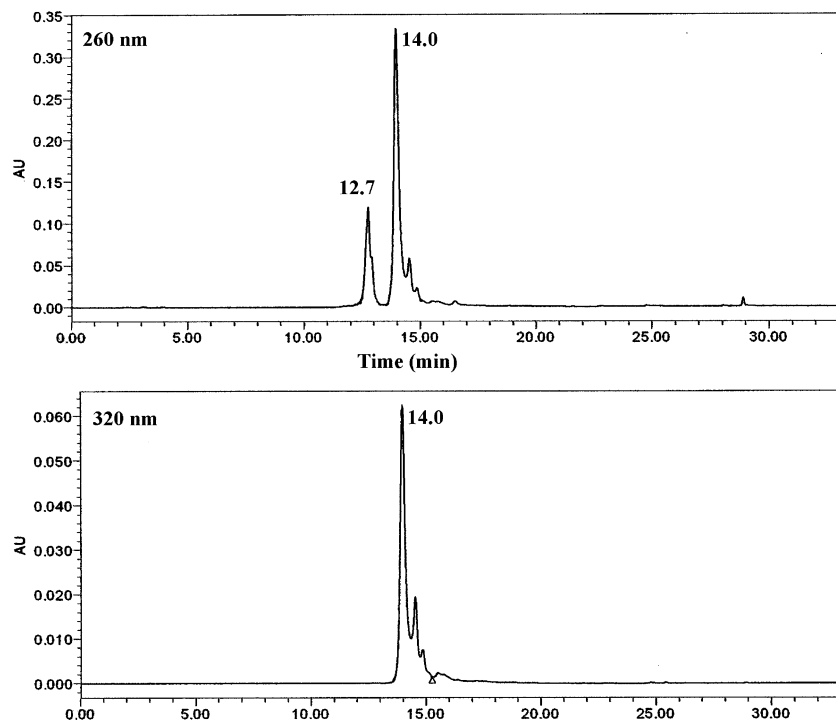
Fig. 2 HPLC profiles (detection at 260 nm (A) and 320 nm (B)) of the crude reaction mixture, after 6 h of reaction of [Ru(ttpy″)$_2$]$^{2+}$ complex **2** with aldehyde functionalized ODN **10a**. Peak (1) with retention time 12.7 min represents the aldehyde functionalized ODN **10a** and the new peak (2) at 14.0 min represents the covalent conjugate **12a**.

6–7 h complete conversion of modified ODNs to the metal–ODN conjugates **12a–d** (ruthenium series) and **13a–d** (iron series) was observed (Fig. 2 depicts as an example the HPLC analysis of a crude coupling reaction mixture). It should be noted that due to the mild conditions employed for the coupling reaction, no

degradation of the metal complex moieties was observed. All the final metal complex–ODN conjugates **11–13** were characterized by mass spectrometry and UV-Vis spectroscopy which showed characteristic bands from ODN (λ_{max} = 260 nm), the terpyridine moiety (λ_{max} = 280 and 320 nm) and metal complexes such as

This journal is © The Royal Society of Chemistry 2009

Org. Biomol. Chem., 2009, **7**, 2729–2737 | 2731

Table 1 Melting temperatures[a] determined at different concentrations of sodium chloride

Duplex sequences	Schematic representation of duplexes	T_m / °C[b], 40 mM	T_m / °C, 100 mM	T_m / °C, 500 mM	ΔT_m / °C[c], 40 mM	ΔT_m / °C, 100 mM	ΔT_m / °C, 500 mM
14a/14b		32.0	36.7	47.1	—	—	—
11a/14b		32.3	37.0	47.6	0.3	0.5	0.5
11a/11b		35.9	41.0	51.7	3.9	4.3	4.6
12a/2-equiv.14b		33.0	39.7	49.0	1.0	1.6	1.9
12a/2-equiv.11b		36.6	41.2	51.7	4.6	4.5	4.6
13a/2-equiv.11b		36.6	41.2	51.7	4.6	4.5	4.6

[a] Optical melts were generated in 0.01 M tris-HCl buffer containing the relevant concentrations of NaCl, pH 7.4 with [duplex conc.] = 1.3×10^{-6} M. [b] T_m were done in duplicate independent melting experiments. The error is within ±0.5 °C. [c] ΔT_m corresponds to the difference in T_m between the modified and unmodified duplex (**14a/14b**) forms.

characteristic MLCT bands either from the Fe(II) complex at $\lambda_{max} = 567$ nm or Ru(II) complex at $\lambda_{max} = 490$ nm.

Hybridization study

The different metal complex–ODN hybrids were hybridized with their respective complementary ODN stretches in 10 mM Tris-HCl buffer at pH = 7 with particular NaCl concentrations. Those duplexes were studied by UV-melting experiments, circular dichroism spectroscopy, and non-denaturing gel electrophoresis.

## Melting temperature analysis (Table 1)

The hybridization properties of the conjugates **11a–b**, **12a** and **13a** as well as other non-modified ODNs **14a** and **14b** were investigated by UV-melting temperature measurements (T_m) by following the changes in absorbance at 260 nm as a function of temperature from 10–80 °C. The study was carried out to evaluate the influence of covalent coupling of the metal complex with the oligonucleotides and the impact on the stability of the duplex DNA by introducing one, two or more metal complexes into the duplex ODN stretches.

It is interesting to note that for duplexes containing a single metal complex (*i.e.* **11a/14b**, **12a/2-equiv. 14b**) no significant change of the duplex stability was observed with respect to the unmodified duplex form (**14a/14b**). On the other hand, the introduction of either two or three metal complexes into duplex DNA stretches, (**11a/11b**) and (**12a/2-equiv. 11b**) respectively, enhances duplex melting temperature by 4–5 °C as compared to the unmodified duplex (**14a/14b**). No hysteresis was observed during the heating and cooling process of the duplex melting, suggesting reversible duplex formation kinetics. Duplex melting was also examined at various NaCl concentrations (40, 100, 500 mM) to analyze the electrostatic effect of metal complex on T_m enhancement. It was observed that on increasing salt concentration, the T_m values for all the duplexes were increased (Table 1). An increase in bulk salt concentration should lead to the stabilization of the duplex state of DNA by having a higher charge density as compared to the single stranded form. This

would result in an increase in T_m for the helix-to-coil transition. But the change in salt concentration does not alter significantly the enhancement of melting temperature (ΔT_m) of modified duplexes with respect to the unmodified one. It should be noted that no difference between ruthenium and iron modified duplexes, (**12a/2-equiv.11b**) and (**13a/2-equiv.11b**) respectively, was observed. Thus, the enhancement in the melting temperature is likely due to the presence of positively charged either Ru(II) or Fe(II) centers into ODN stretches. The melting temperature study thus showed that the introduction of multiple metal complexes in a linear network formed by hybridization does not reduce the stability of the so-formed duplex.

Circular dichroism analysis (Fig. 3)

Circular dichroism spectroscopy may give information about the structure of DNA while incorporating metal complexes into single stranded and duplex ODN stretches. Free Fe(II) and Ru(II) metal complexes **1–3** do not exhibit optical activity and are therefore CD-silent. However, their incorporation in either single stranded ODN or double stranded nucleic acid induces CD signals near to the absorption region of both terpyridine and metal complexes. This kind of induced circular dichroism (ICD) signal is very much dependent on the position of the metal complex that is either at the middle or terminal of the ODN stretches. The single stranded metal complex–ODN conjugates **11a**, **12a** and **13a** exhibit a +ve CD band at 274 nm and a −ve CD band at 250 nm, which indicate possession of some kind of secondary structure (Fig. 3A). It is interesting to note that mono ODN conjugated metal complex **11a** solution shows a structured −ve ICD band at 314 nm, which is close to the terpyridine absorption region, along with a +ve CD band at 488 nm, which is close to the MLCT absorption band of the Ru(II) complex. On the contrary, bis-ODN conjugated metal complex **12a** does not show any ICD band either at the terpyridine or metal complex region. The above CD results indicate that chirality was transferred from ss-ODN stretch to the covalently attached metal complex whereas the chirality induced by ss-ODN to the central
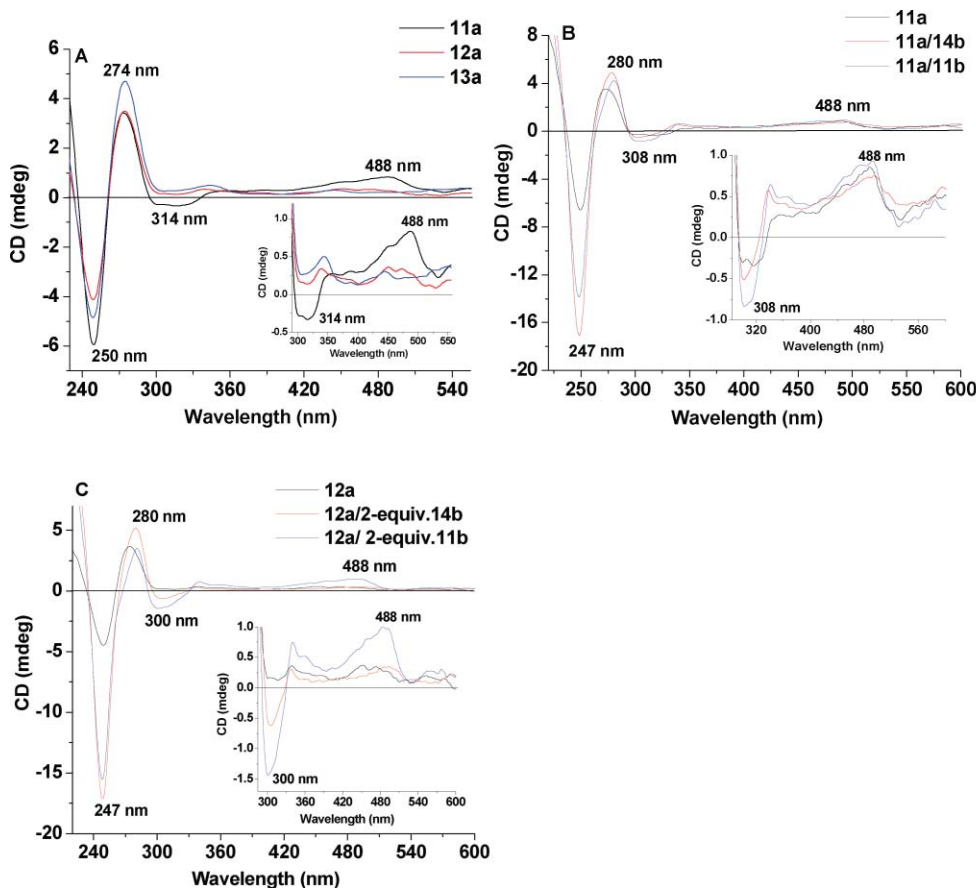
Fig. 3 CD spectra of single stranded metal–ODN hybrids (A) and the duplexes with mono-ODN tethered metal complex (B) and bis-ODN tethered metal complex (C). The respective complementary ODN stretches were carried out in 10 mM tris-HCl, 40 mM NaCl buffer at pH = 7.4 with [single stranded] = [duplex] = 1.3×10^{-6} M concentration. The inset of each figure shows a wider view of ICD bands arising from terpyridine and the metal complexes.

metal complex of bis-ODN–metal hybrids such as **12a**, was almost cancelled out probably due to its centro-symmetric nature.

All kinds of duplexes (**11a/14b**, **11a/11b**, **12a**/2-equiv. **14b**, **12a**/2-equiv. **11b**, **13a**/2-equiv. **11b**, see schematic representation in Table 1) showed a characteristic +ve CD band at 280 nm and a −ve CD band at 248 nm, which is the signature of the B-form of duplex DNA (Fig. 3B and 3C). The duplex formed between the bis-ODN attached metal complex and the corresponding unmodified complementary ODN (**12a**/2-equiv. **14b**) does show the characteristic bands of B-DNA and an additional weak ICD band at 310 nm close to the terpyridine absorption region but no such ICD band was observed near to the MLCT band of the Ru(II) complex (Fig. 3C). On the contrary, the duplex formed by the bis-ODN tethered metal complex with two equivalents of the mono ODN tethered metal complex (**12a**/2-equiv. **11b**) does show characteristic ICD bands (at 300 nm and 488 nm) both from the terpyridine moiety and the metal complex. The resultant duplex seems to be centro-symmetric but a different orientation of the terminally tethered metal complex may be responsible for developing an induced CD band near the MLCT band of the metal complex. All double stranded motifs comprising mono ODN conjugated metal complexes (**11a/14b** and **11a/11b**) showed characteristic ICD bands at 308 nm and 488 nm near the absorption region of the terpyridine and the metal complex

respectively (Fig. 3B), which further proves the significant role of the terminally attached metal complex in developing an ICD band near the absorption region of the metal complex.

Non-denaturing gel electrophoresis (Fig. 4)

The different hybridization products were visualized on polyacrylamide gel electrophoresis (PAGE) in non-denaturating conditions with both AT and GC-rich ODNs. Both sequences resulted in similar kinds of gel bands but the higher stability of the GC-rich nanostructures afforded clearer and more intense gel bands than the AT-rich sequences. Simple hybridization products of bis-ODN attached metal complexes with the respective unmodified complementary ODN stretches (*i.e.* **12c/14d**, **12d/14c**) gave rise to bands with electrophoretic mobilities matched with those of the duplex ODN stretches as assigned by molecular weight markers. The self-assembly process was then explored by hybridizing two complementary bis-ODN tethered metal complexes bearing the same metal (*i.e.* **12c/12d**) or different metals (*i.e.* **12c/13d**). In principle their association can result in controlled linear DNA arrays where the length can be altered by changing the ratio of the two different ODN stretches. In this study, 4 : 1, 2 : 1 and 1 : 1 ratios were used. Two types of hybridization conditions were employed to study such DNA self assembly processes, as we have
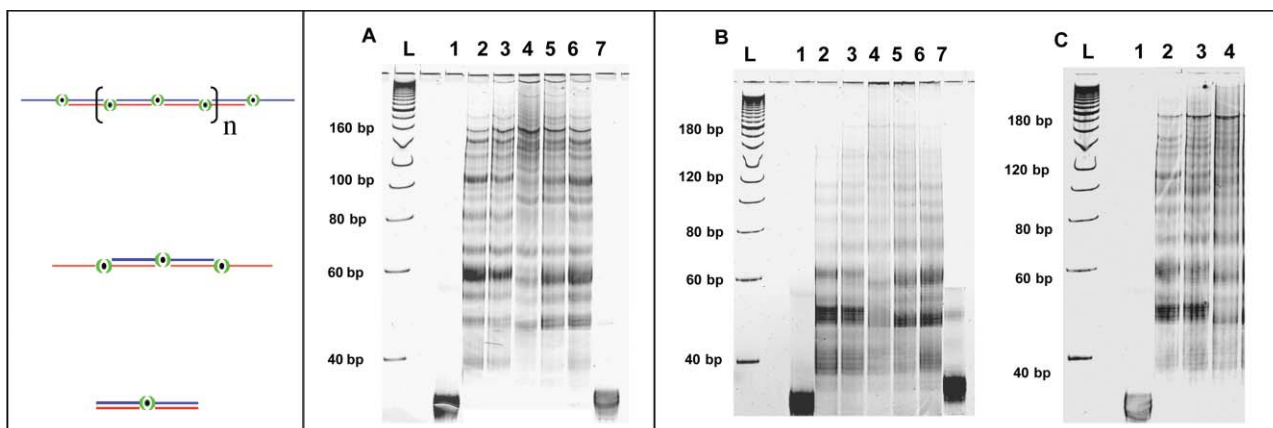
Fig. 4 Non-denaturing PAGE analysis of hybridization products using different ratios of bis-ODN conjugated metal complexes **12c** and **12d** (A) and **12c** and **13d** (B, C). (A) L: 200 bp ladder, lane 1: **12c** + excess complementary unmodified ODN **14d**, lane 2–6: metal–ODN hybrids **12c** and **12d** in ratios of 4 : 1, 2 : 1, 1 : 1, 1 : 2 and 1 : 4, lane 7: **12d** + excess complementary unmodified ODN **14c**. Hybridization was done by heating the solution at 60 °C for 4 min followed by incubation at 4 °C for 24 h. (B) L: 200 bp ladder, lane 1: **12c** + excess complementary unmodified ODN **14d**, lane 2–6: metal–ODN hybrids **12c** and **13d** in ratios of 4 : 1, 2 : 1, 1 : 1, 1 : 2 and 1 : 4, lane 7: **13d** + excess complementary unmodified ODN **14c**. Hybridization was done by incubating the solution at 17 °C for 24 h followed by incubation at 4 °C for 12 h. (C) L: 200 bp ladder, lane 1: **12c** + excess complementary unmodified ODN **14d**, lane 2–4 : metal–ODN hybrids **12c** and **13d** in ratios of 4 : 1, 2 : 1, 1 : 1. In this case hybridization was done by incubating the solution at 50 °C for 3 min followed by incubation at 4 °C for 12 h. The minimum concentration of bis-ODN conjugated metal hybrid used in all of these studies was 10 μM in 20 μl buffer (10 mM tris-HCl and 100 mM NaCl) solution at pH = 7.4. The gel was visualized by EtBr staining.

dealt with both an inert $[Ru(ttpy'')_2]^{2+}$ complex and a relatively labile $[Fe(ttpy'')_2]^{2+}$ complex. In the case of the ruthenium complex, different ratios of **12c** and **12d** were heated at 60 °C for 3 min in 10 mM tris-HCl and 100 mM NaCl buffer followed by incubation at 4 °C for 12 h. In the presence of the more labile iron complex, different ratios of **12c** and **13d** ODN solutions were incubated at 17 °C for 24 h and heated at 50 °C for 3 min followed by incubation at 4 °C for 24 h. Interestingly, when the self assembly was carried out under mild conditions, it was more likely to form one major discrete product along with a small amount of polymeric species. On the other hand, heating at high temperature kinetically allows the formation of a wide range of molecular weight based products as observed in Fig. 4a.

By using an excess of one strand (*i.e.* **12c/12d** with ratios 4 : 1 and 1 : 4, Fig. 4A, lanes 2 and 6), a major band is observed corresponding to about 60 base-pair products. This band can be attributed to the duplex forming between two **12c** ODN stretches with one of its complementary ODNs **12d** and two **12d** ODN stretches with one of its complementary ODNs **12c**, respectively (see schematic representation in Fig. 4). However, it should be noted that distribution of all other higher base-pair linear DNA arrays was also observed. A large distribution of all different kinds of DNA nanostructures ranging from 60 bp to 160 base-pairs were obtained while mixing **12c** and **12d** in 2 : 1 ratios (Fig. 4A, lane 3 and lane 5). More interestingly, one type of higher molecular weight oligomeric species of approximately 160 base-pairs dominated while mixing **12c** and **12d** in a 1 : 1 ratio (Fig. 4A, lane 4).

In this regard, it should be really interesting to linearly align two different metal complexes (*i.e.* Ru(II) and Fe(II)) with different redox potential values by using a simple duplex hybridization property. Using this strategy, the objective is to place alternately, Ru(II) and Fe(II) metals at regular distances along linear ODN stretches to afford multimetallic DNA nanostructures. The above

hybridization conditions were used while incorporating alternating Fe(II) and Ru(II) complexes in a linear DNA array (Fig. 4B and 4C). However, mild hybridization conditions result in less intense higher DNA base pair containing bands as compared to the bands obtained while heating at 60 °C as shown in Fig. 4B and 4C (lanes 4). Gel retardation assays thus proved the formation of higher ordered linear DNA networks with a combination of either similar or different metal complexes by hybridizing two complementary bis-ODN–metal complex conjugates in a 1 : 1 ratio.

Transmission electron microscopy study (Fig. 5)

A preliminary TEM study of negatively stained samples was used to characterize the long linear DNA networks. For these experiments, 1 : 1 and 4 : 1 ratios of **12a/12b** were used. Interestingly, by using a 1 : 1 ratio, the TEM analysis revealed rod-like filaments with lengths around 200 nm with a low polydiversity. In contrast, TEM analysis of hybridization samples with a 4 : 1 ratio did not reveal any filaments, which is probably due to the short length of nanostructures formed in this case. These preliminary results correlated very well with the PAGE analysis and thus demonstrated the formation of high molecular weight oligomeric species in the case of a 1 : 1 ratio.

Conclusions

Here we have shown the synthesis of different oxyamine based metal complexes and their easy and efficient solution phase coupling with 3′-modified ODN stretches (*i.e.* AT and GC-rich). Interestingly, such metal complex–ODN hybrid networks stabilized the duplex form by 1–4 °C as compared to the unmodified duplex moiety. The positive charge of the metal complexes is expected to contribute to the stabilization of various duplexes. A further circular dichroism study proves the
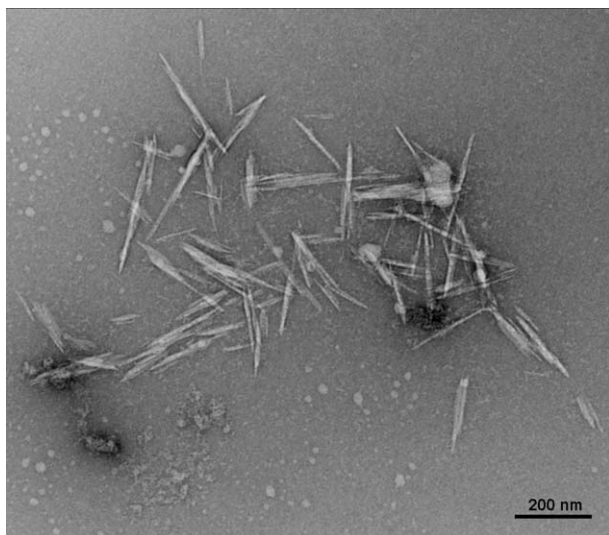
Fig. 5 TEM observation of a hybridization solution of **12a/12b** at a 1 : 1 ratio. Structures were visualized after negative staining. The scale bar corresponds to 200 nm.

formation of a B-DNA duplex between metal complex–ODN conjugates and the respective complementary ODN stretches. The chirality transfer from ss-DNA to the metal complex is another interesting phenomenon obtained from this study. These metal complex–DNA conjugates give us the opportunity to form supramolecular linear DNA nanoassemblies, which remain stable at room temperature and give us access to form multimetallic structures where either similar or different metal complexes can be placed at regular intervals along the ODN stretch. Placement of such different metal complexes with different redox potentials and optical absorption properties should open a new path in developing different nanoelectronics, biosensors and redox stimulated molecular light switches. In principle, such photoactive metal centers separated by DNA double strands can influence each other's photophysical and redox properties depending on the nature of the intervening ODN sequence where Fe(II) will act as an energy or electron trap/sink in polymetallic arrays. In this context, work on the preparation of more luminescent metal complexes, such as an iridium complex, is now underway. Current work also focusses on employing these metal complex–ODN building blocks for successive immobilizations on surfaces and studying the electrochemical properties of each deposited layer by QCM-D.

Experimental section

Materials and methods

All solvents and reagents used were of the highest purity available. N-Boc-O-(carboxymethyl)-hydroxylamine and 4′-tolyl-2,2′:6′,2″-terpyridine (ttpy) were purchased from Aldrich. The starting ligand 4-(aminomethylphenyl)-2,2′:6′,2″-terpyridine **4** and [Ru(ttpy)Cl₃] were synthesized as reported earlier.[9] The solid support 3-[(4,4′-dimethoxytrityl)-glyceryl-1-succinyl] long chain alkylamino CPG was purchased from Eurogentec. Automated synthesis of oligodeoxynucleotides (ODNs) was carried out on an ABI-3400 DNA synthesizer (Applied Biosystems) by using standard β-cyanoethyl phosphoramidite protocols at a 1 μmol

scale. The diol containing oligonucleotides **9a–d** were purified on a μ-Bondapak C-18 column (Macherey-Nagel Nucleosil: 10 × 250 mm, 7 μm) using the following system of solvents: solvent A, 20 mM ammonium acetate–CH_3CN, 95 : 5 (v/v); solvent B (CH_3CN); flow rate, 4 ml min⁻¹; a linear gradient from 0 to 30% B in 20 min was applied. The oligonucleotide conjugates **11–13** were purified by both denaturing polyacrylamide gel electrophoresis (PAGE) and C-18 preparative HPLC using the above conditions. Mass spectra were measured on an Esquire 3000 (Bruker) for ESI and on a MALDI TOF (Bruker). ¹H and ¹³C NMR spectra were recorded on Bruker 300 Spectrometer. Chemical shifts δ are reported in ppm downfield from the internal standard (TMS).

Ligand synthesis

4′-(4-N-(*tert*-Butoxycarbonyl)glycinamidomethylphenyl)-2,2′:6′,2″-terpyridine (ttpy″) 5. To a solution of **4** (300 mg, 0.9 mmol) in CH_2Cl_2 (5 mL), the N-hydroxysuccinimide ester of N-Boc-O-(carboxymethyl)-hydroxylamine (330 mg, 1.17 mmol) was added and the reaction mixture was stirred for 6 h at room temperature. The white precipitate obtained during the course of the reaction was filtered and the filtrate diluted by adding ethyl acetate. The ethyl acetate fraction was washed successively with H_2O, saturated Na_2CO_3 and an additional time with H_2O. The organic phase was dried over Na_2SO_4 and evaporated under vacuum to give **5** as a white solid (300 mg, 65%). ¹H-NMR ($CDCl_3$, 300 MHz) δ 1.4 (s, 9H), 4.37 (s, 2H), 4.56 (d, J = 6 Hz, 2H), 7.3 (ddd, J = 7.4, 4.5, 0.8 Hz, 2H), 7.4 (d, J = 8.4 Hz, 2H), 7.8–7.88 (m, 4H), 8.67 (d, J = 8.0 Hz, 2H), 8.7–8.72 (m, 4H); m/z (DCI) 512.1 (100%, (M + H)⁺), 456 (15, (M − tBu)⁺); Anal. Calcd for $C_{29}H_{29}N_5O_4$·1H₂O: C, 65.77; H, 5.90; N, 13.22%. Found C, 65.67; H, 5.92; N, 12.69%.

Synthesis of complexes

Protected [Fe(ttpy″)₂]²⁺ complex 6. To a solution of **5** (20 mg, 0.04 mmol) and Et₃N (10 μl, 0.07 mmol) in a degassed CHCl₃–EtOH solution (1 : 2, v/v, 5 mL), FeCl₂·4H₂O (4.8 mg, 0.024 mmol) was added. An immediate purple coloration was observed and the resultant solution was stirred under nitrogen for 1 h at room temperature. Ethanol was next added and the solution was centrifuged. The supernatant was concentrated, dissolved in a minimum amount of ethanol and precipitated from cold acetone. The precipitate was centrifuged, washed several times with acetone followed by tetrahydrofuran to afford pure complex **6** (28 mg, 70%). ¹H-NMR (CD_3OD, 300 MHz) δ 1.5 (s, 9H), 4.4 (s, 2H), 4.6 (s, 2H), 7.2 (t, J = 7.0 Hz, 2H), 7.3 (d, J = 5.6 Hz, 2H), 7.8 (d, J = 8.7 Hz, 2H), 8.0 (t, J = 7.5 Hz, 2H), 8.4 (d, J = 8 Hz, 2H), 8.9 (d, J = 7.7 Hz, 2H), 9.5 (s, 2H); ¹³C-NMR (CD_3OD, 75 MHz) δ 28.5 (CH_3), 43.4 (CH_2), 76.6 (CH_2), 83.2 (quat), 122.5 (CH), 125.3 (CH), 128.7 (CH), 129.2 (CH), 129.9 (CH), 136.8 (quat), 140.0 (CH), 142.8 (quat), 152.0 (quat), 154 (CH), 159.6 (quat), 161.8 (quat), 171.7 (quat); m/z (ESI) 539.1 (M²⁺/2); UV (λ nm, CH_3CN) 567, 319, 307, 285.

Protected [Ru(ttpy″)₂]²⁺ complex 7. Compound **5** (113 mg, 0.22 mmol), ruthenium trichloride hydrate (20 mg, 0.096 mmol) and AgNO₃ (0.05 g, 0.3 mmol) were added to a degassed CHCl₃–EtOH solution (1 : 2, v/v, 20 mL) and the mixture was heated to reflux under nitrogen overnight. The mixture was filtered and the

This journal is © The Royal Society of Chemistry 2009

Org. Biomol. Chem., 2009, **7**, 2729–2737 | **2735**

residue chromatographed on silica gel (eluent: CH_3CN–H_2O–sat. KNO_3, 40 : 1 : 1, v/v/v). Fractions containing the product were combined and the solvent removed under vacuum. Excess KNO_3 was filtered off from a CH_3CN solution to obtain the red colored final complex **7** (75 mg, 30%). ^{1}H-NMR (CD$_3$CN, 300 MHz) δ 1.45 (s, 9H), 4.4 (s, 2H), 4.6 (s, 2H), 7.1 (ddd, J = 7.5, 6.6, 1.2 Hz, 2H), 7.43 (d, J = 5.2 Hz, 2H), 7.66 (d, J = 8.3 Hz, 2H), 7.94 (ddd, J = 8.7, 7.7, 1.5 Hz, 2H), 8.18 (d, J = 8.3 Hz, 2H), 8.67 (d, J = 7.8 Hz, 2H), 9.03 (s, 2H); ^{13}C-NMR (CD$_3$CN, 75 MHz) δ 28.0 (CH$_3$), 42.6 (CH$_2$), 76.0 (CH$_2$), 82.7 (quat), 122.2 (CH), 125.2 (CH), 128.1 (CH), 128.6 (CH), 129.3 (CH), 136.3 (quat), 138.7 (CH), 142.2 (quat), 148.7 (quat), 153.1 (CH), 156.1 (quat), 158.9 (quat), 170.1 (quat); m/z (ESI) 562.1 (M^{2+}/2); UV (λ nm, CH$_3$CN) 490, 310, 285.

Protected [Ru(ttpy'')(ttpy)]$^{2+}$ complex 8. A mixture of [Ru(ttpy)Cl$_3$] (100 mg, 0.14 mmol), compound **5** (70 mg, 0.14 mmol) and AgNO$_3$ (57 mg, 0.33 mmol) were added into a degassed CHCl$_3$–EtOH solution (1 : 2, v/v, 5 ml) and the resultant solution was heated at reflux under nitrogen for 8 h. The red solution was then filtered, evaporated under vacuum and the residue chromatographed on a silica gel column (eluent CH$_3$CN–H$_2$O–sat. KNO$_3$, 40 : 0.5 : 0.5, v/v/v). Fractions containing the product were combined and the solvent was removed. Excess KNO$_3$ was filtered off from a CH$_3$CN solution to finally obtain **8** as a red colored solid in 40% yield (50 mg). ^{1}H-NMR (CD$_3$CN, 300 MHz) δ 1.44 (s, 9H), 2.5 (s, 3H), 4.35 (s, 2H), 4.6 (s, 2H), 7.14–7.19 (m, 4H), 7.4–7.44 (m, 4H), 7.54 (d, J = 8.0 Hz, 2H), 7.65 (d, J = 8.2 Hz, 2H), 7.92 (ddd, J = 7.8, 1.4 Hz, 4H), 8.1 (d, J = 8.2 Hz, 2H), 8.17 (d, J = 8.3 Hz, 2H), 8.68 (d, J = 8.2 Hz, 4H), 9.0 (s, 4H); ^{13}C-NMR (CD$_3$CN, 75 MHz) δ 21.1 (CH$_3$), 28.1 (CH$_3$), 42.8 (CH$_2$), 76.2 (CH$_2$), 82.9 (quat), 122.1 (CH), 122.3 (CH), 125.4 (CH), 128.0 (CH), 128.4 (CH), 128.7 (CH), 129.4 (CH), 131.1 (CH), 134.8 (quat), 136.6 (quat), 138.8 (CH), 141.9 (quat), 142.1 (quat), 148.9 (quat), 149.4 (quat), 153.1 (CH), 156.3 (quat), 156.4 (quat), 159.1 (quat), 170.7 (quat); m/z (ESI) 468.0 (M^{2+}/2); UV (λ nm, CH$_3$CN) 490, 310, 284.

Complex 1. Boc protected [Fe(ttpy'')$_2$]$^{2+}$ complex **6** (10 mg, 9.3 µmol) was dissolved in CH$_3$CN–1 N HCl (1 : 1, v/v, 2 mL) and the reaction mixture was stirred for 2 h at room temperature. The resultant solution was evaporated and dried in vacuum to obtain the violet colored [Fe(ttpy'')$_2$]$^{2+}$ complex **1** in 80% yield (7.0 mg). ^{1}H-NMR (D$_2$O, 300 MHz) δ 4.4 (s, 2H), 4.6 (s, 2H), 7.1 (t, J = 6.8 Hz, 2H), 7.25 (d, J = 5.6 Hz, 2H), 7.76 (d, J = 7.9 Hz, 2H), 7.9 (t, J = 7.8 Hz, 2H), 8.3 (d, J = 7.8 Hz, 2H), 8.6 (d, J = 7.9 Hz, 2H), 9.24 (s, 2H); m/z (ESI) 439.0 (M^{2+}/2); UV (λ nm, CH$_3$CN) 580, 291.

Complex 2. The cleavage of the Boc protecting group on complex **7** was carried out under the same conditions as for **6** to afford the complex **2** in 80% yield. ESI-MS: m/z (ESI) 461.9 (M^{2+}/2); UV (λ nm, CH$_3$CN) 490, 314, 285.

Complex 3. The cleavage of the Boc protecting group on complex **8** was carried out under the same conditions as for **6** to afford complex **3** in 80% yield. m/z (ESI) 417.0 (M^{2+}/2); UV (λ nm, CH$_3$CN) 490, 310, 284.

Oligonucleotide synthesis

The oligonucleotides **10a–d** functionalized at the 3'-end by an aldehyde group were prepared following a previously reported protocol by using a post-synthetic oxidation of a diol moiety.[10]

General procedure for the coupling reaction between oligonucleotides and metal (Ru^{2+} and Fe^{2+}) complexes

(A) Coupling of mono ODN to [Ru(ttpy)(ttpy'')]$^{2+}$ complex 3: conjugates 11a–d. To a solution (300 µl) of aldehyde-containing oligonucleotide **10a** (1.0 mg, 0.19 µmol) in 0.4 M ammonium acetate buffer (pH = 4.5), an aqueous solution of mono-oxyamino containing Ru^{2+} metal complex **3** (0.4 mg, 0.47 µmol) was added so that the final concentration of the metal complex remained at ~0.02 M. The resultant reaction mixture was stirred at room temperature. The reaction was followed by RP-HPLC, which indicates almost 100% consumption of **10a** into conjugate **11a** within a 2 h time period. The crude product was purified either by reverse phase HPLC or by 30% denaturing gel electrophoresis to afford the final conjugate **11a** in ~40% (460 µg) isolated yield. m/z (MALDI) calcd 6093.5, found 6085.3. Conjugates **11b**, **11c** and **11d** were obtained using a similar protocol.

(B) Coupling of bis-ODNs to [Ru(ttpy'')$_2$]$^{2+}$ complex 2: conjugates 12a–d. Aldehyde functionalized ODN **10b** (1.0 mg, 0.19 µmol) was dissolved in 0.4 M ammonium acetate buffer solution (300 µl, pH = 4.5) and an aqueous solution of bis-oxyamino containing metal complex **2** (85 µg, 0.09 µmol) was added dropwise in 3 steps. The progress of the reaction was followed by reverse phase HPLC. After complete addition of the metal complex the reaction mixture was left overnight. This process actually converts all aldehyde functionalized ODN into the bis-ODN tethered metal complex, **12b**. The crude product was purified by reverse phase HPLC to afford final bis-ODN–metal complex conjugate **12b** in 35% isolated yield. m/z (MALDI) calcd 11566.3, found 11545.8. Conjugates **12a**, **12c** and **12d** were obtained using a similar protocol.

(C) Coupling of bis-ODNs to [Fe(ttpy'')$_2$]$^{2+}$ complex 1: conjugates 13a–d. Conjugates **13a–d** were obtained using a similar protocol as for **12a–d**. **13b** m/z (MALDI) calcd 11521.2, found 11499.1.

UV-melting experiment

The modified single stranded metal–ODN conjugate (1.3 µM) was mixed with the appropriate concentrations of the complementary ODN stretches in 10 mM tris-HCl buffer at pH = 7.4 by varying the salt concentrations (e.g. 40, 100 and 500 mM NaCl). In one case the hybridization was carried out by heating the ODN mixtures at 60 °C for 3 min followed by incubation at 4 °C for 24 h. Modified duplexes with ODNs containing the Fe(II) complex were incubated at 17 °C for 24 h and heated at 50 °C for 3 min followed by incubation at 4 °C for 12 h. The stability of such modified hybrid duplexes was compared with the respective unmodified duplexes by thermal denaturation experiments. The melting experiments were acquired on a CARY 400 Scan UV-Vis spectrophotometer equipped with a temperature programmable cell-block, by following the changes in absorbance at 260 nm as a function of temperature ranging from 10–80 °C. The samples were heated at 1.0 °C per min and the absorbance values were recorded

for every 1 °C rise in temperature. All T_m experiments were carried out twice in the above mentioned NaCl buffer solutions. The average melting temperature value for two independent melting experiments is mentioned in Table 1.

Circular dichroism spectroscopy

CD spectra were recorded using a JASCO (J-810) model spectropolarimeter equipped with a Perkin-Elmer temperature controller. The experiments were carried out in 40 mM NaCl, 0.01 M tris-HCl buffer at pH 7.4 using 1.3 µM duplex concentrations at 25 °C. All CD scans were averaged over at least 3 acquisitions from 220–650 nm and the scan rate was maintained at 50 nm per min with optical cells wit a path length of 1 cm. All the CD values were expressed as ellipticity ($A_L - A_R$) in millidegrees.

Native non-denaturing gel electrophoresis

Samples were prepared by combining different ratios of two complementary bis-ODN tethered metal complexes each at 10 µM concentration in 10 mM tris-HCl and 100 mM NaCl at pH = 7.4. There were two major hybridization experimental conditions, in one case hybridization was done by heating the solution at 60 °C for 3 min followed by incubation at 4 °C for 24 h and in the other case hybridization was done by incubating the solution at 17 °C for 24 h followed by incubation at 4 °C for 12 h. Native PAGE (15%) containing 1 × tris-borate buffer was used to analyze the samples. All samples (20 µl) were diluted with 5 µl of 40% glycerol prior to loading on the gel. The gel was cooled to 5 °C by circulating ice-cold water across the gel plate prior to use. Electrophoresis was carried out for 6–8 h at 10–15 °C. This condition should maintain the stability of the supramolecular self assembled DNA hybrids during their migration through the gel. All bands in the gels were detected by using ethidium bromide stains.

Transmission electron microscopy

The solutions of double strands **12a/12b** were heated at 60 °C in 10 mM tris-HCl and 100 mM NaCl buffer followed by incubation at 4 °C for 48 hours. A tiny drop of the hybridization solution of **12a/12b** at a different ratio was deposited onto glow-discharged carbon-coated TEM grids. A drop of 2% (w/v) uranyl acetate negative stain was added prior to complete drying. After 3 min, the liquid in excess was blotted and the remaining film was allowed to dry. The specimens were observed using a Philips CM200 microscope operated at 80 kV. Images were recorded on Kodak S0163 films at a magnification of 15000.

References

1 K. V. Gothelf and T. H. LaBean, *Org. Biomol. Chem.*, 2005, **3**, 4023–4037; N. C. Seeman, *Mol. Biotechnol.*, 2007, **37**, 246–257; F. C. Simmel, *Angew. Chem., Int. Ed.*, 2008, **47**, 5884–5887; C. M. Niemeyer, *Curr. Opin. Chem. Biol.*, 2000, **4**, 609–618; J. J. Storhoff and C. A. Mirkin, *Chem. Rev.*, 1999, **99**, 1849–1862.
2 N. C. Seeman, *Angew. Chem., Int. Ed.*, 1998, **37**, 3220–3228.
3 *For DNA linear networks*: P. W. K. Rothemund, *Nature*, 2006, **440**, 297–302; S. M. Waybright, C. P. Singleton, K. Wachter, C. J. Murphy and U. H. Bunz, *J. Am. Chem. Soc.*, 2001, **123**, 1828–1833. *For triangular assembly*: J. S. Choi, C. W. Kang, K. Jung, J. W. Yang, Y.-G. Kim and H. Han, *J. Am. Chem. Soc.*, 2004, **126**, 8606–8607; N. Chelyapov, Y. Brun, M. Gopalkrishnan, D. Reishus, B. Shaw and L. Adleman, *J. Am. Chem. Soc.*, 2004, **126**, 13924–13925. *For tetrahedral assembly*: R. P. Goodman, R. M. Berry and A. J. Turberfield, *Chem. Commun.*, 2004, 1372–1373; R. P. Goodman, I. A. T. Schaap, C. F. Tardin, C. M. Erben, R. M. Berry, C. F. Schmidt and A. J. Turberfield, *Science*, 2005, **310**, 1661–1665; N. Mitchell, R. Schlapak, M. Kastner, D. Armitage, W. Chrzanowski, J. Riener, P. Hinterdorfer, A. Ebner and S. Howorka, *Angew. Chem., Int. Ed.*, 2009, **48**, 525–527. *For hexagonal assembly*: J. Tumpane, R. Kumar, E. P. Lundberg, P. Sandin, N. Gale, I. S. Nandhakumar, B. Albinsson, P. Lincoln, L. M. Wilhelmsson, T. Brown and B. Norden, *Nano Lett.*, 2007, **7**, 3832–3839.
4 H. Yang and H. F. Sleiman, *Angew. Chem., Int. Ed.*, 2008, **47**, 2443–2446; D. Mitra, N. Di Cesare and H. F. Sleiman, *Angew. Chem., Int. Ed.*, 2004, **43**, 5804–5808; I. Vargas-Baca, D. Mitra, H. J. Zulyniak, J. Banerjee and H. F. Sleiman, *Angew. Chem., Int. Ed.*, 2001, **40**, 4629–4631; K. M. Stewart, J. Rojo and L. W. McLaughlin, *Angew. Chem., Int. Ed.*, 2004, **43**, 5808–5811; K. M. Stewart and L. W. McLaughlin, *J. Am. Chem. Soc.*, 2004, **126**, 2050–2057; K. M. Stewart and L. W. McLaughlin, *Chem. Commun.*, 2003, 2934–2935.
5 H. C. Kolb, M. G. Finn and K. B. Sharpless, *Angew. Chem., Int. Ed.*, 2001, **40**, 2004–2021.
6 P. M. E. Gramlich, C. T. Wirges, A. Manetto and T. Carell, *Angew. Chem., Int. Ed.*, 2008, **47**, 8350–8358.
7 Y. Singh, N. Spinelli and E. Defrancq, *Curr. Org. Chem.*, 2008, **12**, 263–290; E. Garanger, D. Boturyn, O. Renaudet, E. Defrancq and P. Dumy, *J. Org. Chem.*, 2006, **71**, 2402–2410; S. Ghosh, E. Defrancq, J. Lhomme, P. Dumy and S. Bhattacharya, *Bioconjugate Chem.*, 2004, **15**, 520–529.
8 M. Maestri, N. Armaroli, V. Balzani, E. C. Constable and A. M. W. Cargill Thompson, *Inorg. Chem.*, 1995, **34**, 2759–2767.
9 O. Johansson, M. Borgström, R. Lomoth, M. Palmblad, J. Bergquist, L. Hammarström, L. Sun and B. Åkermark, *Inorg. Chem.*, 2003, **42**, 2908–2918.
10 O. P. Edupuganti, Y. Singh, E. Defrancq and P. Dumy, *Chem.–Eur. J.*, 2004, **10**, 5988–5995.

This journal is © The Royal Society of Chemistry 2009

Org. Biomol. Chem., 2009, **7**, 2729–2737 | 2737